UV-Induced Ligand Exchange in MHC Class I Protein Crystals

Patrick H.N. Celie[1], Mireille Toebes[2], Boris Rodenko[3], Huib Ovaa[3], Anastassis Perrakis[1,] and Ton N.M. Schumacher[2,*]*

The Netherlands Cancer Institute, Plesmanlaan 121, 1066 CX, Amsterdam, The Netherlands.

[1]Division of Biochemistry, [2]Division of Immunology, [3]Division of Cell Biology II,

p.celie@nki.nl, m.toebes@nki.nl, b.rodenko@nki.nl, h.ovaa@nki.nl

*Corresponding Authors: a.perrakis@nki.nl, t.schumacher@nki.nl

Running Title: In Crystallo Exchange of MHC Class I ligands

Abstract: High-throughput structure determination of protein-ligand complexes is central in drug development and structural proteomics. To facilitate such high-throughput structure determination we designed an induced replacement strategy. Crystals of a protein complex bound to a photosensitive ligand are exposed to UV light, inducing the departure of the bound ligand, allowing a new ligand to soak in. We exemplify the approach for a class of protein complexes that is especially recalcitrant to high-throughput strategies: the MHC class I proteins. We developed a UV-sensitive, "conditional", peptide ligand whose UV-induced cleavage in the crystals leads to the exchange of the low-affinity lytic fragments for full-length peptides introduced in the crystallant solution. This "*in crystallo*" exchange is monitored by the loss of seleno-methionine anomalous diffraction signal of the conditional peptide

compared to the signal of labeled MHC β2m subunit. This method has the potential to facilitate high-throughput crystallography in various protein families.

Introduction

High-throughput (HTP) structure determination of protein-ligand complexes is central to understanding the nature of protein-ligand interactions and for drug development.[1] In typical HTP protein-ligand X-ray crystallography, crystals of the ligand-free protein or of a low affinity protein-inhibitor complex are soaked in a solution with the novel inhibitor to obtain the complex structure. This allows typically hundreds of structures to be determined in a more or less straightforward manner. However, for many protein families it is not possible to obtain crystals of the protein alone or with a low affinity inhibitor that can be easily displaced.

A protein family noticeably recalcitrant to high throughput crystallography has been that of MHC class I proteins. MHC class I molecules bind eight to eleven amino acid peptides derived from endogenous and pathogen-encoded proteins for subsequent display at the cell membrane. This 'presentation' of peptide-MHC complexes at the surface of all nucleated cells allows cytotoxic T cells to monitor cells for alterations in the cellular proteome that occur upon infection with pathogens. When cytotoxic T cells detect the presence of a foreign peptide-MHC complex, this results in T cell activation and subsequent killing of the infected cell. The amino-acid sequence requirements for peptide binding to MHC class I molecules are loose, and it is estimated that approximately one out of every two hundred peptides can bind with high affinity. Consequently, the number of different peptide epitopes from endogenous and pathogen-derived proteins that have to be distinguished by cytotoxic T cells is vast.

Crystallographic analysis of peptide-MHC (pMHC) complexes has contributed substantially to our understanding of the nature of T cell recognition. Seminal work by Bjorkman and colleagues provided the first view of the molecular complex seen by T cells,[2] and subsequent work has extended this to other antigens and to TCR-pMHC complexes.[3] In spite of these efforts, the fraction of the pMHC repertoire for which structural data is available remains small and this limits both our understanding of the

biophysical basis of T cell specificity and the development of immunomodulatory strategies. For instance, only about half of the pathogen-derived peptide repertoire that is presented by MHC molecules induces detectable cytotoxic T cell responses;[4] however the structural requirements that make a foreign pMHC complex into an immunogenic pMHC complex remain unknown. Secondly, while the potential value of sequence variants of tumor-associated peptide antigens with improved MHC binding properties has been tested in a series of clinical trials,[5,6] our understanding of the effect of structural changes induced by such sequence alterations is incomplete.[7] Finally, taking into account recent efforts for the high-throughput mapping of T cell epitopes in major human pathogens,[7-11] the parallel development of a more comprehensive structural view of the pMHC repertoire is desirable. A major bottleneck for HTP structure determination of pMHC complexes, is the need to refold MHC together with individual peptides and optimize crystallization conditions for each new complex. Furthermore, classical soaking strategies are not applicable, as the peptide-free ('empty') MHC molecule is unstable and hence refractory to crystallization.[12-14]

Light induced strategies for the study of reaction mechanisms in protein crystals have been extensively used, notably and mostly in the context of kinetic studies.[15-17] Here we present a method that is also based on light-induced chemical reactions, but with the aim to generate structures of novel complexes within the existing crystal. This method is based on the use of peptide tools we have recently described (Figure 1),[18-20] and makes pMHC complexes amenable to HTP X-ray crystallographic analysis. Specifically, using MHC molecules bound to non-natural MHC ligands that contain UV-sensitive nitrophenyl groups (modified amino-acids denoted J_1 and J_2), exposure to UV light can be used to cleave MHC bound ligands. As the peptide fragments formed after cleavage have a much reduced affinity for the MHC peptide binding groove, these low-affinity fragments can be exchanged for a new higher-affinity ligand in solution.

Here we describe the structure of the MHC complex with a conditional MHC class I ligand and a structure of the partly empty MHC complex produced upon UV-induced cleavage of the ligand. We then demonstrate the value of UV-induced replacement soaking of peptides "*in crystallo*" for the structural

analysis of defined pMHC complexes. Finally, we exemplify the use of the seleno-methionine anomalous diffraction signal of labeled conditional ligands and MHC proteins as an internal control for the efficiency of *in crystallo* ligand exchange reactions.

Materials and Methods

Construction of synthetic peptides. All peptides were synthesized by standard Fmoc (9-fluorenyl-methylcarbonyl) synthesis. Fmoc-derivatives of the UV-light sensitive building blocks J_1 ((2-nitro)phenylglycine) and J_2 (3-amino-3-(2-nitro)phenyl-propionic acid) were prepared as described.[18]

Purification of HLA-A2.1 – peptide complexes. HLA-A2.1 heavy chain was expressed in *E. coli* BL21 (DE3) plysS and human β2m was expressed in *E. coli* XL1 Blue cells. Seleno-methionine containing β2m was produced in minimal medium complemented with amino-acids and seleno-methionine instead of methionine. HLA molecules were refolded in the presence of peptide KILGJ_2VFJ_1V or Se-MILGJ_2VFJ_1V. Subsequently, pMHC complexes were purified by gel-filtration chromatography on a Phenomex Biosep S3000 column in 20 mM Tris-HCl (pH 7.0) and 150 mM NaCl. The complex was loaded on a Mono-Q anion exchange column and eluted with a NaCl gradient in 20 mM Tris-HCl (pH 7.0). Final preparations were stored at 4 °C.

Crystallization. Prior to crystallization screening, protein buffer was exchanged to 20mM MES (pH 6.5) using a Centriprep concentrator. 200 nL sitting drops (100 nL protein + 100 nL crystallization solution) were prepared in 96-well crystallization plates using the Mosquito crystallization robot and were screened against the PACT crystallization screen.[21] Well-diffracting crystals were finally grown from 20 – 24% PEG 1500, 0.1 M MES-NaOH (pH 6.0 – 6.5) using microseeding in 4 µl hanging drops (2 µl protein + 2 µl crystallization solution) at 20 °C.

HLA-A2.1:KILGJ_2VFJ_1V crystals were frozen in 30 % PEG 1500, 10 % glycerol, 0.1 M MES-NaOH (pH 6.5). HLA-A2.1:Se-MILGJ_2VFJ_1V crystals were frozen in 25 % PEG 1500, 15 % glycerol, 0.1 M MES-NaOH (pH 6.5). Cryogenic solutions were slowly added to the crystals in at least three steps to

equilibrate the crystals against the glycerol-containing solutions. Crystals were mounted in SPINE pins, vitrified in liquid nitrogen and stored until data collection.

Peptide exchange in MHC crystals. To examine cleavage of MHC-bound UV-sensitive peptides, HLA-A2.1:KILGJ$_2$VFJ$_1$V (or :Se-MILGJ$_2$VFJ$_1$V) crystals were transferred to 4 µl drops of crystallization solution positioned within the sub-wells of a 96-well Greiner Crystal Quick Low-Profile crystallization plates. For peptide exchange experiments, crystals were transferred to 4 µl crystallization solution containing 2.5 or 5 mM peptide from 100 mM stocks in DMSO. The resulting final concentration of 2.5-5 % DMSO did not measurably affect crystal stability. In all cases, 75 µl of crystallization solution was then added to the reservoir well to minimize evaporation during UV exposure. Crystallization plates containing multiple drops with crystals were exposed 3-6 times to UV light (366 nm UV lamp, 2x15W blacklight blue tubes, LxWxH 505x140x117 mm, Uvitec, UK, 10 cm distance from sample) for 10 minutes at 4 °C, with 2 minutes intervals to minimize temperature increase and evaporation. After UV irradiation, plates were sealed with Hampton ClearSeal prior to further usage and stored for 3 to 24 hrs at 20 °C, allowing cleaved peptide fragments to dissociate and/or to be exchanged for the newly added ligand.

Data collection, processing and structure refinement. Diffraction data were collected using synchrotron radiation at the ESRF and the SLS. All crystals belong to the monoclinic space group P2$_1$, with a β angle close to 90^o degrees. In the case of the Se-substituted peptide, crystals have dramatically different morphology and are pseudo-merohedrally twinned, although the lattice changes are minute. Data was collected on single crystals for each of the structures. Data for HLA2.1: KILGJ$_2$VFJ$_1$V (intact and UV-cleaved) was collected at a wavelength of 1.072 Å; data for HLA-A2.1:ILKEPVHGV at 0.973 Å; data for HLA-A2.1:KLTPLCVTL, HLA-A2.1:Se-MILGJ$_1$VFJ$_2$V, HLA-A2.1:NLVPMVATV and HLA-A2.1(Se-Mβ2m):AMDSNTLEL at 0.979 Å and data for HLA-A2.1(Se-Mβ2m):Se-MILGJ$_1$VFJ$_2$V at a wavelength of 0.978 Å. All diffraction data were integrated by MOSFLM[22] and scaled in SCALA[23], keeping an identical free reflection set for R_{free} validation wherever possible. Molecular replacement using an HLA-2.1 structure with the ligand removed was performed with AMORE through the CCP4i

interface.[24] For all complexes following the complex with the conditional ligand we first used our refined model of the HLA2.1: KILGJ_2VFJ_1V in the absence of the ligand for molecular replacement. The two molecules in the asymmetric unit were not NCS restrained owing to the relatively high resolution and the fact that we observed at least in some cases differences between the two molecules. In all cases the positioned models were refined in REFMAC[25]. Manual inspection, rebuilding and the placement of the peptides was done with Coot[26]. Restrain libraries for non-standard amino-acids were created in the CCP4i sketcher and LIBCHECK. Final refinement was performed in PHENIX[27] to allow refinement of the twin fraction, and group occupancy refinement for the peptide moiety. All structures have R_{free} below 26.2 % , were validated in Coot and WHATCHECK[28] and are submitted to the PDB.

Results

Structure of a conditional ligand - MHC class I complex. To allow efficient release of peptide fragments generated upon UV exposure of MHC crystals, a new conditional ligand, KILGJ_1VFJ_2V, was designed for the human MHC class I protein HLA-A2 (where J_1 is (2-nitro)phenylglycine as described[18] and J_2 is 3-amino-3-(2-nitro)phenyl-propionic acid.[29] Because of the presence of two UV-sensitive groups, UV-induced cleavage of this ligand results in formation of three short peptide fragments that each have a low affinity for MHC class I, and this is expected to facilitate fragment release from the protein within crystals (Figure 1A).

We first crystallized the complex between this new, optimized conditional ligand and the HLA-A2.1 protein and solved the crystal structure (see supplementary data, Table S1 for statistics). During all crystallographic experiments the structure was solved using the HLA2.1 structure without a bound peptide or other ligand as a model, to minimize bias. The unliganded structures were first refined and the peptide was then modeled in the σ_A-weighted electron density maps and the complex structures were refined. The HLA-A2.1:KILGJ_1VFJ_2V structure exhibits a typical MHC class I fold[2,30] with the peptide located within the well characterized peptide-binding groove between two α-helices from the α1 and α2

domains of the heavy chain (Figure 2A-C). The electron density maps for the peptide are clear, except for the 'side chains' of residues J_2 and J_1, which are not well defined (Figure 2D).

In crystallo **cleavage of conditional ligands bound to MHC class I.** To test the feasibility of UV-induced cleavage of bound peptide ligands in MHC class I crystals, but also to see if we could obtain the structure of a (partially) "empty" MHC class I molecule, we subjected HLA-A2.1:KILGJ_1VFJ_2V crystals to UV irradiation prior to vitrification and X-ray data collection. In the resulting structure (Figure 2E), the electron density for residues 5-7 (J_1VF), between the two cleavage sites has largely disappeared. This implies that cleavage has occurred at both sites and that the central part of the peptide has dissociated from the MHC class I protein. Notably, peptide residues Lys-1 to Gly-4 (KILG) and Val-9 remain bound in almost identical positions as in the non-exposed structure. Crystallographic refinement of the occupancy of the remaining peptide residues converged to above 92% (Table S1) and demonstrates that the majority of the MHC class I molecules in the crystal remain associated with peptide fragments 1 and 3. Following cleavage, J_2 should remain connected to Val 9 but we did not model it into the structure since the density clearly suggests that J_2 is disordered after cleavage (Figure 2E). The elimination of the central part of the peptide has no significant effect on the overall structure of the HLA-A2.1 structure (rmsd value of 0.33 Å between 375 Cα atoms) (Figure S1). Apparently, the remaining peptide residues and crystal contacts are capable of maintaining the integrity of the HLA-A2.1 structure within the crystal. The only significant local changes in the HLA-A2.1 protein is that Arg-97 and Tyr-116, which display double conformations in the liganded structure, adopt only a single conformation after UV exposure (Figure 3C,D).

Collectively, these data show that UV-induced cleavage of an MHC-bound peptide in pMHC crystals occurs efficiently and that the central peptide fragment is liberated from the structure. Based on these results, we decided it would be meaningful to attempt an exchange of the UV-cleavage products with newly added peptide ligands.

In crystallo **peptide exchange.** We selected two known HIV-1 derived HLA-A2 restricted epitopes for these experiments. The ILKEPVHGV peptide is derived from HIV-1 reverse transcriptase (RT_{468-}

$_{476}$). The crystal structure of this peptide in complex with HLA-A2.1 is known (PDB code 1HHJ[30]), and could serve as a validation for our method. The KLTPLCVTL is derived from the HIV-1 envelope ($Env_{120-128}$) and its structure was not known.

HLA-A2.1:KILGJ$_2$VFJ$_1$V crystals were exposed to UV-light in the presence of either the $Env_{120-128}$ or $RT_{468-476}$ peptide for 30 to 60 minutes, and after at least 3hrs of 'back-soak', crystals were vitrified and used for X-ray diffraction analysis. High-resolution structures were obtained for both crystals (Table S1 for details). The electron density maps, which were calculated in the absence of any peptide to minimize bias, clearly indicated that ligand exchange was successful. Both peptides were modeled and the structures were refined; the resulting electron density maps are shown in Figure 3.

The electron density for the ILKEPVHGV epitope is well defined and residues Ile-1, Gln-4 and His-7 are clear indicators of peptide exchange (Figure 3A). Occupancy refinement shows that more than 70% of the molecules in the crystal contain this peptide. Superposition of our HLA-A2.1:ILKEPVHGV structure onto the published HLA-A2.1:ILKEPVHGV structure (PDB code 1HHJ) indicates that the exchanged peptide adopts an identical conformation to the one observed in 1HHJ (rmsd = 0.29 Å, Figure S2). This suggests that the *in crystallo* peptide exchange results in a physiologically relevant structure, similar to the one obtained by refolding, as expected.

The electron density for the KLTPLCVTL peptide in exchanged HLA-A2 crystals is also well defined except for the side chains of Val-5 and Cys-6. In particular the density of Pro-4, Val-7 and Leu-9 support the notion that ligand exchange has occurred upon UV exposure (Figure 3B). Occupancy refinement shows that about 79% of the MHC molecules are occupied by the newly added ligand. Notably, the orientation of Arg-97 and Tyr-116 in the HLA-A2.1:KLTPLCVTL structure is distinct from that in the ILKEPVHGV and KILGJ$_2$VFJ$_1$V complexes, consistent with the presence of the bulkier Leu-9 side chain[30] providing an independent indicator of successful ligand exchange. These data demonstrate that *in crystallo* ligand exchange is a feasible strategy for high-throughput analysis of pHLA structures.

An internally controlled procedure for *in crystallo* peptide exchange. For high-throughput applications it would be of value to introduce an internal control to quantify the efficiency of ligand

exchange in the final structure. A validation method would be particularly advantageous in cases where exchange would only occur in a fraction of the molecules within the crystal or when peptides that closely resemble the conditional peptide are used.

We designed a new UV-sensitive ligand, Se-MILGJ$_1$VFJ$_2$V, in which the N-terminal Lys was replaced by a seleno-methionine residue (Se-M). The N-terminal residue should be tolerant to such a change according to MHC class I binding prediction algorithms. Moreover, since the peptide fragment containing this residue remains bound to the MHC class I complex when no new ligand is present during UV exposure (see Figure 1C), a loss of signal should indicate replacement of the UV-induced fragment by the newly added ligand rather than just UV-induced cleavage of the first ligand.

The structure of HLA-A2.1:Se-MILGJ$_1$VFJ$_2$V was solved first (Figure 4A,B). The anomalous difference electron density map shows the presence of the selenium atom (Figure 4A and Table S2). As expected, the Se-M side chain is well ordered (Figure 4B) and the peptide adopts a conformation virtually identical to that in the HLA-A2.1:KILGJ$_1$VFJ$_2$V structure.

HLA-A2.1:Se-MILGJ$_1$VFJ$_2$V crystals were then exposed to UV light in the presence of a third known HLA-A2.1 ligand, the Cytomegalovirus (CMV) pp65$_{495\text{-}503}$ epitope (NLVPMVATV). The structure of HLA-A2.1:NLVPMVATV was solved using a diffraction data collection and processing procedure identical to the Se-MILGJ$_1$VFJ$_2$V structure. Within this electron density map, the selenium signal has disappeared (Figure 4C) while the electron density matches the NLVPMVATV sequence, demonstrating that peptide exchange was also successful for this ligand (Figure 4D). Crystallographic refinement suggests 93 % occupancy of the NLVPMVATV peptide in the binding pocket, implying that measurement of the anomalous selenium signal provides a suitable method for determining the *in crystallo* exchange efficiency of MHC class I bound peptides.

To provide an estimate for the efficiency of the exchange reaction, we further optimized the validation procedure by crystallizing HLA-A2.1(Se-Mβ2m):Se-MILGJ$_1$VFJ$_2$V using MHC β2m protein in which both the N-terminal and C-terminal methionine residues are replaced by Se-M residues. After X-ray data collection at the appropriate wavelength, the anomalous signal for the selenium atoms in both the β2m

and the Se-Met peptide can be measured. Upon UV-induced peptide exchange within these crystals, the selenium signal from the Se-Met in the peptide should be reduced, while the signal from the Se-M β2m should not be affected. Therefore, comparison between the signals of the selenium atoms within the peptide and β2m should provide a proper estimate of exchange efficiency (%). The structure of HLA-A2.1(Se-Mβ2m):Se-MILGJ$_1$VFJ$_2$V was solved (Figure 5A-C) and the anomalous difference density levels (in electrons per cubic Ångstrom) for each of the selenium atoms was measured.

Next, we performed an exchange reaction with these crystals, using peptide AMDSNTLEL, an epitope from the H5N1 ('avian flu') Influenza A/Vietnam/1194/04 Nucleoprotein (np$_{373-381}$).[19] Diffraction data was collected for two different crystals and the structures were solved. Comparison of the Se-M signal in the peptide and in the β2m subunit for the HLA-A2.1(Se-Mβ2m):Se-MILGJ$_1$VFJ$_2$V and HLA-A2.1(Se-Mβ2m):AMDSNTLEL structures, indicated that about 44 % of the peptides was exchanged in one of the structures and about 63% in the second structure (for details see Table S2). Indeed, the new peptide could be built with confidence in the electron density of the second HLA-A2.1(Se-Mβ2m):AMDSNTLEL structure (Figure 5D-F). Thus, this optimized validation protocol using Se-M residues in both protein and peptide appears to be an objective and feasible method for determination of ligand-exchange efficiency, and is recommended as a default for future assays.

Discussion

We here demonstrate that *in crystallo* exchange allows the X-ray structure determination of pMHC class I complexes. Using a stock of preformed HLA crystals occupied with a newly designed conditional ligand, MHC crystals containing a desired peptide antigen can be produced in a less than 3hr procedure.

Soaking new (small) ligands into crystals of a ligand-free molecule and removing a low affinity ligand in favor of a new high affinity ligand in protein crystals, has become an accepted method in both industry and academia. In a particular case of CDK2A/CA crystals, peptide ligands bound to the protein could be removed and exchanged for new peptides by passive diffusion over a period of days.[31] A main advantage of such soaking strategies is that it eliminates the requirement for refolding of every single new protein - ligand complex and screening of crystallization conditions.

The low off-rate of bound ligands precludes such a strategy for many molecules, including MHC class I molecules. To nevertheless allow high-throughput structural analysis we have designed conditional peptide ligands of which the affinity for proteins within crystals can be manipulated through UV exposure. This method is simple and allows parallel exposure of multiple MHC - UV-peptide crystals, in the presence of different peptides, resulting in the generation of large collections of defined pMHC crystals with relatively little effort. Furthermore, structure solution is straightforward as virtually no changes in space group and/or unit cell dimensions are observed after the ligand-exchange reaction.

In crystallo peptide exchange was validated in three distinct ways. First, crystal structures with clear electron density were obtained for four out of four cases tested. This included a pMHC complex with a previously known viral antigen, resulting in an exchanged structure that was essentially identical (rmsd 0.29 Å) to the structure obtained by refolding and crystallization; two novel pMHC structures in complex with viral antigens that are presented here; and one pMHC structure containing a non-natural peptide ligand (Rodenko et al. manuscript in preparation). Second, we detect side-chain rearrangements within the MHC, both upon UV cleavage and upon exchange with a new peptide, consistent with previously reported observations.[30] Third, the presence of seleno-methionine within the conditional ligand provides an internal validation for successful peptide exchange, through measurement of the loss

of anomalous signal. This conclusively demonstrates that a significant number of molecules of conditional ligand in the crystal leave upon exchange. This is further verified by incorporation of Se-M residues within the β2m subunit to obtain a reference selenium signal that is not affected by the exchange procedure. Further, IC50 values were determined for all five peptides applied for in crystallo exchange (see supporting information) using a fluorescence polarization assay.[20] For these peptides, ranging from medium (5 < IC50 < 50 μM) to low (IC50 > 50 μM) affinity, efficient exchange (post-exchange occupancy of 70-94%) was achieved without any optimization of ligand concentrations or incubation times.

Solution phase UV-induced exchange of MHC ligands is not restricted to HLA-A2.1[19], but has also proven feasible for HLA-A1, A3, A11, B7[20], the mouse MHC products H-2D^b and K^b, L^d [19, 32, 33] and MHC class II.[34] By analogy, the *in crystallo* exchange technology developed here can likely be extended to a large series of HLA alleles, thereby allowing high-throughput structure analysis of at least one HLA gene product for the majority of individuals. Furthermore, the fact that peptides can be cleaved both in solution and within crystals opens up the possibility to screen for (small) non-peptide ligands that interfere with peptide binding. Identification of such compounds, both functionally and structurally, may prove useful to target specific MHC alleles that are involved in autoimmune diseases or that form targets in MHC mismatched allogeneic transplantation.

The *in crystallo* cleavage and exchange method described here provides a high-throughput strategy for the structural analysis of MHC class I bound ligands. The method is straightforward and applicable in any X-ray structural biology lab. In addition, the usage of UV-cleavable conditional ligands may well be expanded to other ligand-protein complexes, such as MHC Class II complexes, complexes of the regulatory domains of various kinases with peptides, protease-ligand complexes, etc, for which conditional ligands have been[34] or can be defined.

Acknowledgment. We thank Henk Hilkmann for peptide synthesis, Titia Sixma for critically reading this manuscript and Adnane Achour (Karolinska Institute, Sweden) for advice during an early phase of this project. We are grateful to beamline scientists at ESRF (Grenoble, France) and SLS (Villigen, Switserland) for assistance during data collection experiments. This work was supported by LSBR grant 0522 (TNMS), Dutch Cancer Society grant UL 2007-3825 (TNMS) and NWO grant 700.55.422 (HO).

Supporting Information Available: Supplemental data include a table on the data collection and refinement statistics of all structures described, a table with the anomalous difference signals for the selenium atoms, two figures showing superimposed peptides to illustrate the difference/similarity between the respective peptides and a figure showing a the IC_{50} values obtained from a peptide exchange fluorescence polarization (FP) assay.

References

(1) Blundell, T. L.; Jhoti, H.; Abell, C. *Nat Rev Drug Discov* **2002**, *1*, 45-54.

(2) Bjorkman, P. J.; Saper, M. A.; Samraoui, B.; Bennett, W. S.; Strominger, J. L.; Wiley, D. C. *Nature* **1987**, *329*, 512-8.

(3) Garcia, K. C.; Adams, E. J. *Cell* **2005**, *122*, 333-6.

(4) Yewdell, J. W.; Bennink, J. R. *Annu Rev Immunol* **1999**, *17*, 51-88.

(5) Dudley, M. E.; Nishimura, M. I.; Holt, A. K.; Rosenberg, S. A. *J Immunother (1997)* **1999**, *22*, 288-98.

(6) Speiser, D. E.; Lienard, D.; Rufer, N.; Rubio-Godoy, V.; Rimoldi, D.; Lejeune, F.; Krieg, A. M.; Cerottini, J. C.; Romero, P. *J Clin Invest* **2005**, *115*, 739-46.

(7) Borbulevych, O. Y.; Insaidoo, F. K.; Baxter, T. K.; Powell, D. J., Jr.; Johnson, L. A.; Restifo, N. P.; Baker, B. M. *J Mol Biol* **2007**, *372*, 1123-36.

(8) Hosken, N.; McGowan, P.; Meier, A.; Koelle, D. M.; Sleath, P.; Wagener, F.; Elliott, M.; Grabstein, K.; Posavad, C.; Corey, L. *J Virol* **2006**, *80*, 5509-15.

(9) Lewinsohn, D. A.; Winata, E.; Swarbrick, G. M.; Tanner, K. E.; Cook, M. S.; Null, M. D.; Cansler, M. E.; Sette, A.; Sidney, J.; Lewinsohn, D. M. *PLoS Pathog* **2007**, *3*, 1240-9.

(10) Oseroff, C.; Kos, F.; Bui, H. H.; Peters, B.; Pasquetto, V.; Glenn, J.; Palmore, T.; Sidney, J.; Tscharke, D. C.; Bennink, J. R.; Southwood, S.; Grey, H. M.; Yewdell, J. W.; Sette, A. *Proc Natl Acad Sci U S A* **2005**, *102*, 13980-5.

(11) Sylwester, A. W.; Mitchell, B. L.; Edgar, J. B.; Taormina, C.; Pelte, C.; Ruchti, F.; Sleath, P. R.; Grabstein, K. H.; Hosken, N. A.; Kern, F.; Nelson, J. A.; Picker, L. J. *J Exp Med* **2005**, *202*, 673-85.

(12) Bouvier, M.; Wiley, D. C. *Nat Struct Biol* **1998**, *5*, 377-84.

(13) Ljunggren, H. G.; Stam, N. J.; Ohlen, C.; Neefjes, J. J.; Hoglund, P.; Heemels, M. T.; Bastin, J.; Schumacher, T. N.; Townsend, A.; Karre, K.; et al. *Nature* **1990**, *346*, 476-80.

(14) Schumacher, T. N.; Heemels, M. T.; Neefjes, J. J.; Kast, W. M.; Melief, C. J.; Ploegh, H. L. *Cell* **1990**, *62*, 563-7.

(15) Bourgeois, D.; Royant, A. *Curr Opin Struct Biol* **2005**, *15*, 538-47.

(16) Moffat, K. *Acta Crystallogr A* **1998**, *54*, 833-41.

(17) Schlichting, I. *Acc Chem Res* **2000**, *33*, 532-8.

(18) Rodenko, B.; Toebes, M.; Hadrup, S. R.; van Esch, W. J.; Molenaar, A. M.; Schumacher, T. N.; Ovaa, H. *Nat Protoc* **2006**, *1*, 1120-32.

(19) Toebes, M.; Coccoris, M.; Bins, A.; Rodenko, B.; Gomez, R.; Nieuwkoop, N. J.; van de Kasteele, W.; Rimmelzwaan, G. F.; Haanen, J. B.; Ovaa, H.; Schumacher, T. N. *Nat Med* **2006**, *12*, 246-51.

(20) Bakker, A. H.; Hoppes, R.; Linnemann, C.; Toebes, M.; Rodenko, B.; Berkers, C. R.; Hadrup, S. R.; van Esch, W. J.; Heemskerk, M. H.; Ovaa, H.; Schumacher, T. N. *Proc Natl Acad Sci U S A* **2008**, *105*, 3825-30.

(21) Newman, J.; Egan, D.; Walter, T. S.; Meged, R.; Berry, I.; Ben Jelloul, M.; Sussman, J. L.; Stuart, D. I.; Perrakis, A. *Acta Crystallogr D Biol Crystallogr* **2005**, *61*, 1426-31.

(22) Leslie, A. G. W. *Joint CCP4 + ESF-EAMCB Newsletter on Protein Crystallography* **1992**, *26*.

(23) Evans, P. R. *Joint CCP4 and ESF-EACBM Newsletter* **1997**, *33*, 22-24.

(24) CCP4 (Collaborative Computational Project, N. *Acta Crystallogr D Biol Crystallogr* **1994**, *50*, 760-3.

(25) Murshudov, G. N.; Vagin, A. A.; Dodson, E. J. *Acta Crystallogr D Biol Crystallogr* **1997**, *53*, 240-55.

(26) Emsley, P.; Cowtan, K. *Acta Crystallogr D Biol Crystallogr* **2004**, *60*, 2126-32.

(27) Adams, P. D.; Grosse-Kunstleve, R. W.; Hung, L. W.; Ioerger, T. R.; McCoy, A. J.; Moriarty, N. W.; Read, R. J.; Sacchettini, J. C.; Sauter, N. K.; Terwilliger, T. C. *Acta Crystallogr D Biol Crystallogr* **2002**, *58*, 1948-54.

(28) Vriend, G. *J Mol Graph* **1990**, *8*, 52-6, 29.

(29) Bosques, C. J.; Imperiali, B. *J Am Chem Soc* **2003**, *125*, 7530-1.

(30) Madden, D. R.; Garboczi, D. N.; Wiley, D. C. *Cell* **1993**, *75*, 693-708.

(31) Kontopidis, G.; Andrews, M. J.; McInnes, C.; Cowan, A.; Powers, H.; Innes, L.; Plater, A.; Griffiths, G.; Paterson, D.; Zheleva, D. I.; Lane, D. P.; Green, S.; Walkinshaw, M. D.; Fischer, P. M. *Structure* **2003**, *11*, 1537-46.

(32) Grotenbreg, G. M.; Roan, N. R.; Guillen, E.; Meijers, R.; Wang, J. H.; Bell, G. W.; Starnbach, M. N.; Ploegh, H. L. *Proc Natl Acad Sci U S A* **2008**, *105*, 3831-6.

(33) Frickel, E. M.; Sahoo, N.; Hopp, J.; Gubbels, M. J.; Craver, M. P.; Knoll, L. J.; Ploegh, H. L.; Grotenbreg, G. M. *J Infect Dis* **2008**, *198*, 1625-33.

(34) Grotenbreg, G. M.; Nicholson, M. J.; Fowler, K. D.; Wilbuer, K.; Octavio, L.; Yang, M.; Chakraborty, A. K.; Ploegh, H. L.; Wucherpfennig, K. W. *J Biol Chem* **2007**, *282*, 21425-36.

Figure Captions

Figure 1. Cleavage and exchange of UV-sensitive conditional ligands in pMHC complexes. (A) Outline of the general concept of UV-induced ligand exchange. (B) Chemical structure of the UV sensitive $KILGJ_2VFJ_1V$ peptide. (C) Peptide fragments produced following photo-cleavage of $KILGJ_2VFJ_1V$.

Figure 2. Crystal structures of native and UV-exposed HLA-A2.1:$KILGJ_2VFJ_1V$. (A) A cartoon diagram of the overall structure of HLA-A2.1: $KILGJ_2VFJ_1V$ showing the heavy chain (light and dark blue) and β2m (green) as ribbons and the peptide (carbons in yellow, oxygens in red and nitrogens in blue) as sticks. (B) Surface representation of the HLA-A2.1 molecule using the same coloring as in (A), with the bound peptide as a stick model in the same orientation as in (A); the surface is semi-transparent to allow the peptide to be seen inside the peptide binding groove. (C) The same as in (B) but in the view that will be used in subsequent figures and chosen to clearly reveal all differences; this panel is shown to orient the reader (D) The $KILGJ_2VFJ_1V$ peptide in non-exposed HLA-A2.1:$KILGJ_2VFJ_1V$ crystals shown as a stick model together with the final 2mFO-DFc electron density map displayed at a contour level of 1.2 sigma and a radius of 1.8 Å around the peptide. (E) The partial $KILGJ_2VFJ_1V$ peptide in HLA-A2.1:$KILGJ_2VFJ_1V$ crystals after UV cleavage together with the corresponding map, displayed exactly as in (D).

Figure 3. Structures of peptides bound to HLA-A2.1 after *in crystallo* exchange. (A) The ILKEPVHGV peptide is shown as a stick model together with the final 2mFO-DFc electron density map displayed at a contour level of 1.2 sigma and a radius of 1.8 Å around the peptide. (B) The same for the KLTPLCVTL structure. (C-F) the side-chains of the HLA-A2.1 residues Arg-97 and Tyr-116 are shown as sticks (at the top); peptide residues 6 to 9 are also shown as sticks (at the bottom). Carbon atoms in yellow for the

KILGJ$_2$VFJ$_1$V peptide (C), orange for the cleaved KILGJ$_2$VFJ$_1$V after UV exposure (D) green for the exchanged ILKEPVHGV (E) and magenta for the exchanged KLTPLCVTL peptide (F), oxygens in red and nitrogens in blue in all panels. The structure of HLA-A2.1: KILGJ$_2$VFJ$_1$V (C) has been superimposed on the other structures (D – F) and is represented with thin lines for reference, using the same colors as in (C).

Figure 4. Validation of peptide exchange by measuring the anomalous signal of the selenium atoms. (A) Structure of Se-MILGJ$_2$VFJ$_1$V peptide bound to HLA-A2.1 before UV exposure. The anomalous difference Fourier map (with coefficients (F^+-F^-), -$i\alpha$, where (F^+-F^-) are the anomalous difference amplitude, α is the protein phase and -$i\alpha$ corresponds to a rotation of the protein phase by 90^o in the complex plane to account for the fact that $\vec{F}_P$, the protein structure factor, is perpendicular to $\vec{F}^+$ *and* $\vec{F}^-$ structure factors) is shown in grey at the 2.5 sigma contour level and in magenta at the 5.0 sigma contour level, to demonstrate the "noise" level in these maps and in the Se signal respectively; some noise peaks are visible around the Se atom while the Se has a strong signal. (B) Structure of the same Se-MILGJ$_2$VFJ$_1$V peptide as in (A), now with the final 2mFO-DFc electron density map displayed at a contour level of 1.2 sigma and a radius of 1.8 Å around the peptide. (C) Structure of the NLVPMVATV peptide bound to HLA-A2.1 after UV-induced replacement of seMILGJ*VFJV. The map contours clearly show that while some noise peaks with a similar signal as in the previous structure are present, no signal is detected at the location of the Se atom without UV exposure, indicating that the majority of the conditional peptide has indeed been displaced. (D) Same NLVPMVATV peptide as in (C), now with the final 2mFO-DFc electron density map displayed at a contour level of 1.2 sigma and a radius of 1.8 Å around the peptide.

Figure 5. Internal validation of peptide exchange by measuring the anomalous signal of selenium atoms in peptide and β2m. (A) Structure of peptide Se-MILGJ$_2$VFJ$_1$V bound to HLA-A2.1(Se-Mβ2m) before UV exposure with the anomalous difference map (magenta) displayed at the 3.5 sigma contour level. (B) The same peptide as in (A), now with the final 2mFO-DFc electron density map (blue), displayed as described in Figure 4B. (C) N- and C-terminal β2m residues (Se-M residues 0 and 99, respectively) are shown in a stick representation and part of the β2m subunit is shown in ribbon (green). The anomalous difference Fourier map (magenta) is displayed at the 3.5 sigma contour level. (D) Structure of peptide AMDSNTLEL bound to HLA-A2.1(Se-Mβ2m) after exchange with the anomalous difference map (magenta) as described in (A). Carbon atoms are in grey. (E) Same peptide as in (D), displayed with the final 2mFO-DFc electron density map as described in (B). (F) N- and C-terminal β2m residues (Se-M residues 0 and 99, respectively) and part of the β2m chain are displayed with the anomalous difference Fourier map (magenta) as described in (C).

FIGURES

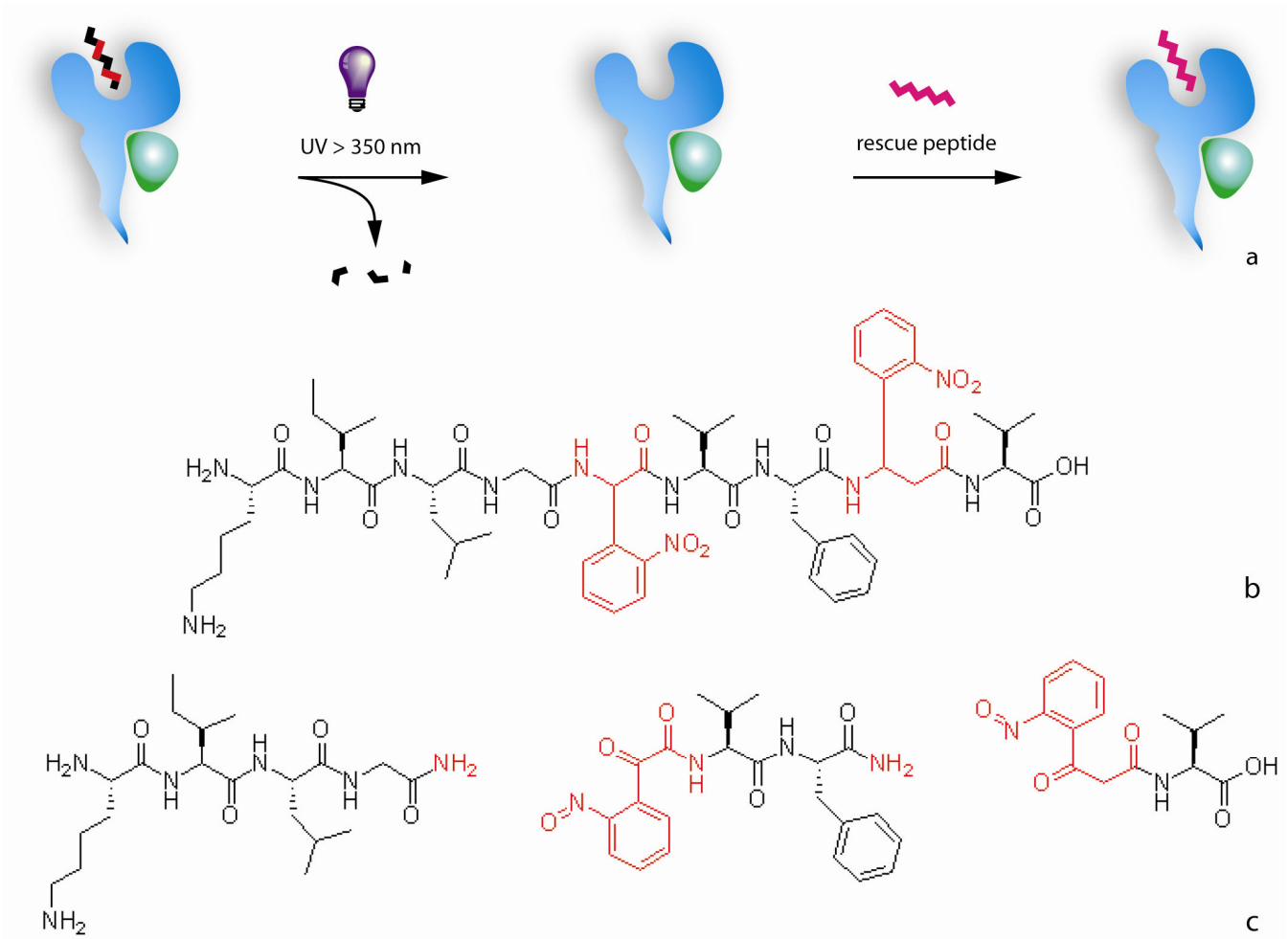

Figure 1 Perrakis/Schumacher

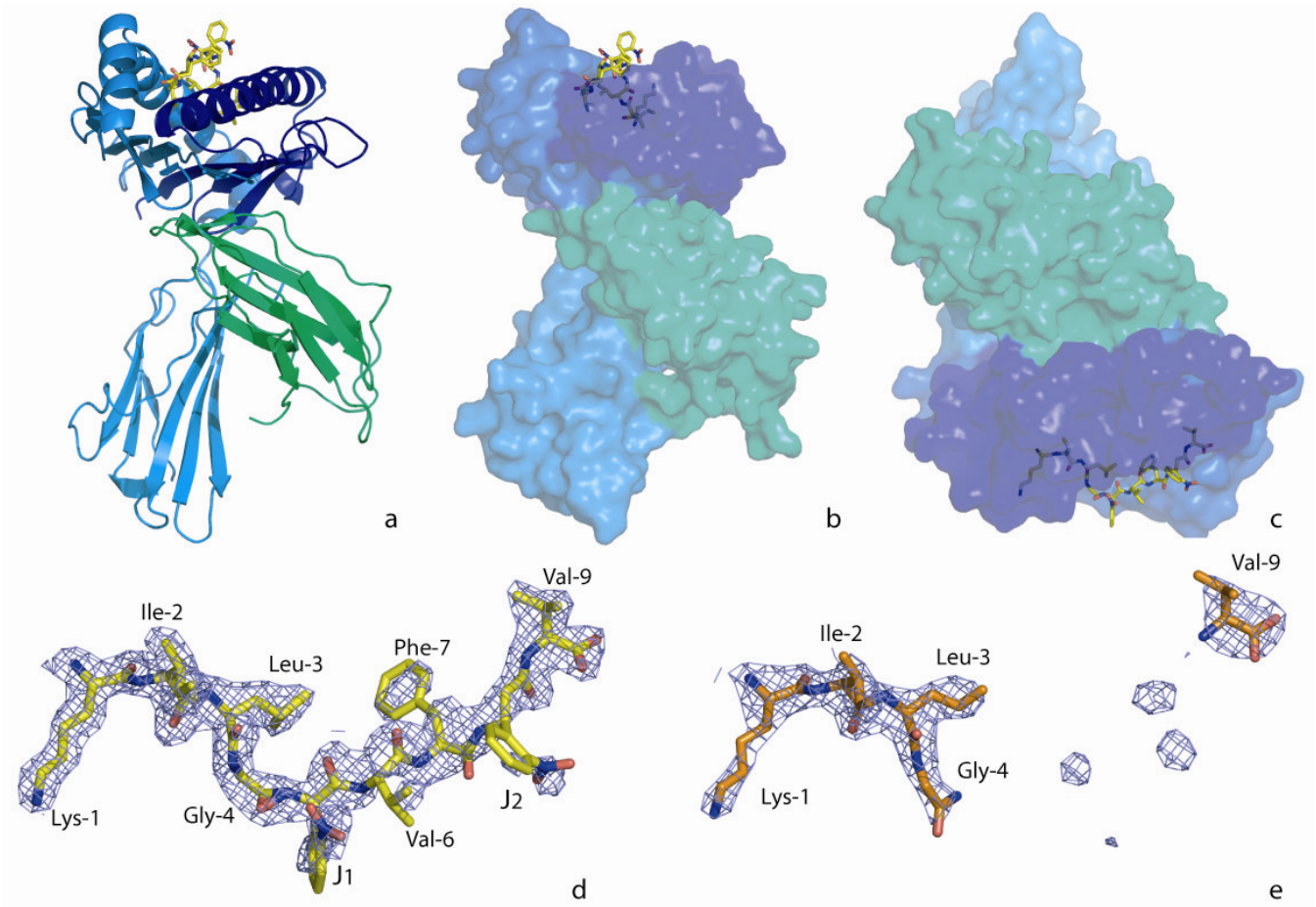

Figure 2 Perrakis/Schumacher

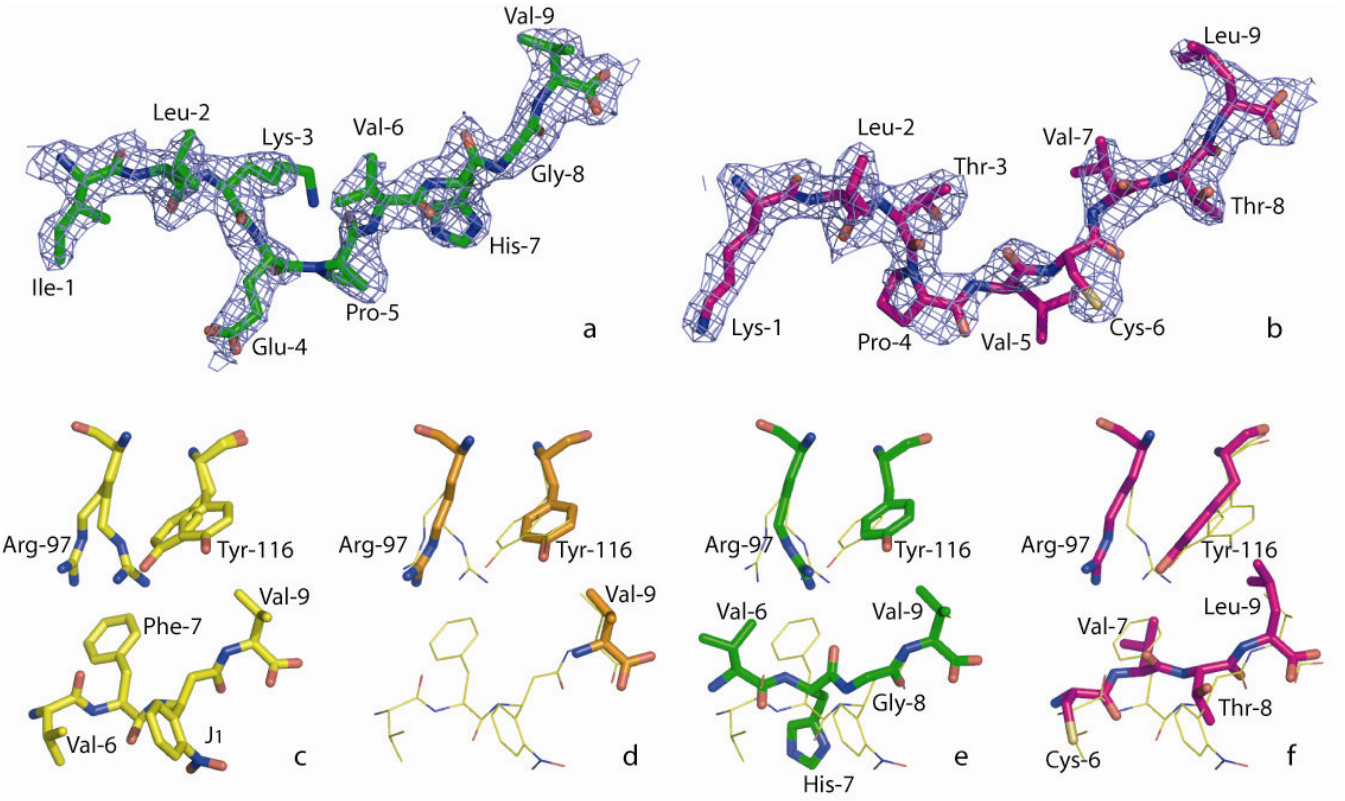

Figure 3 Perrakis/Schumacher

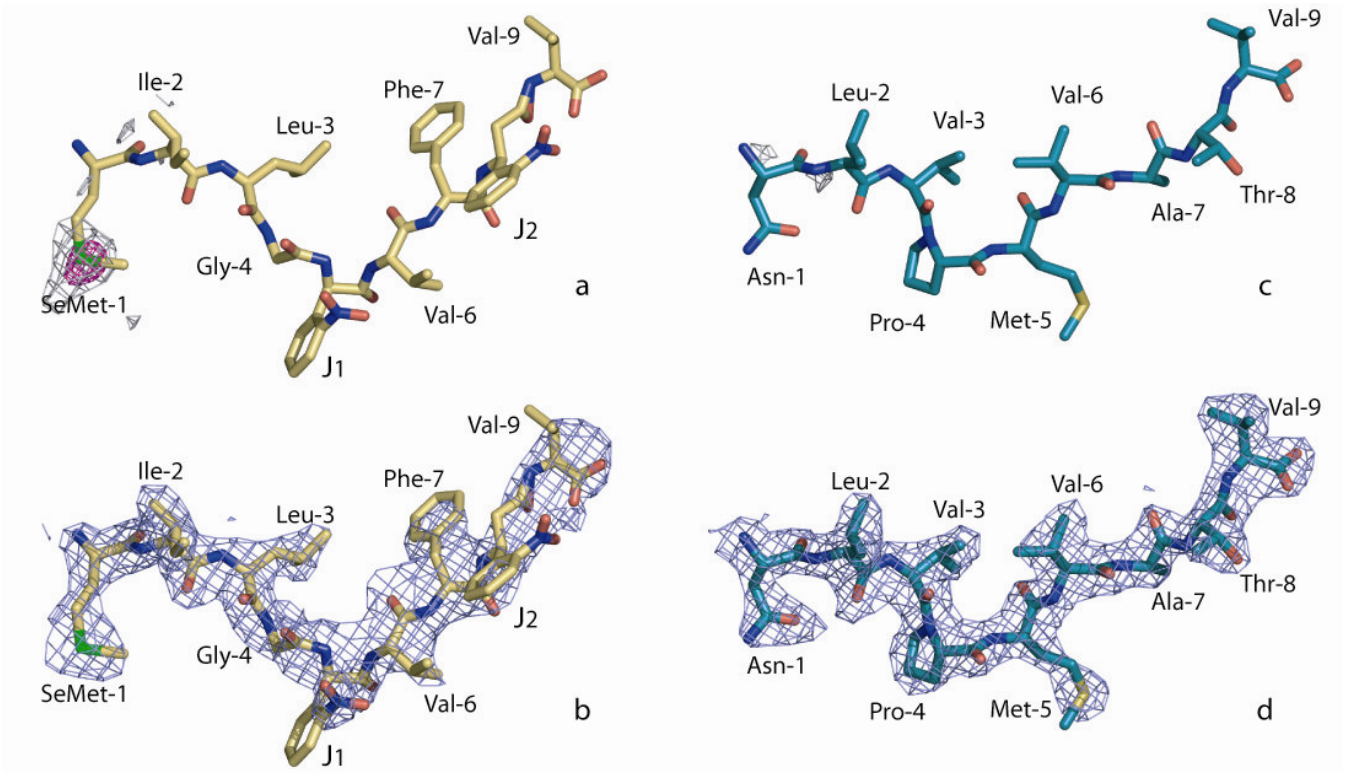

Figure 4 Perrakis/Schumacher

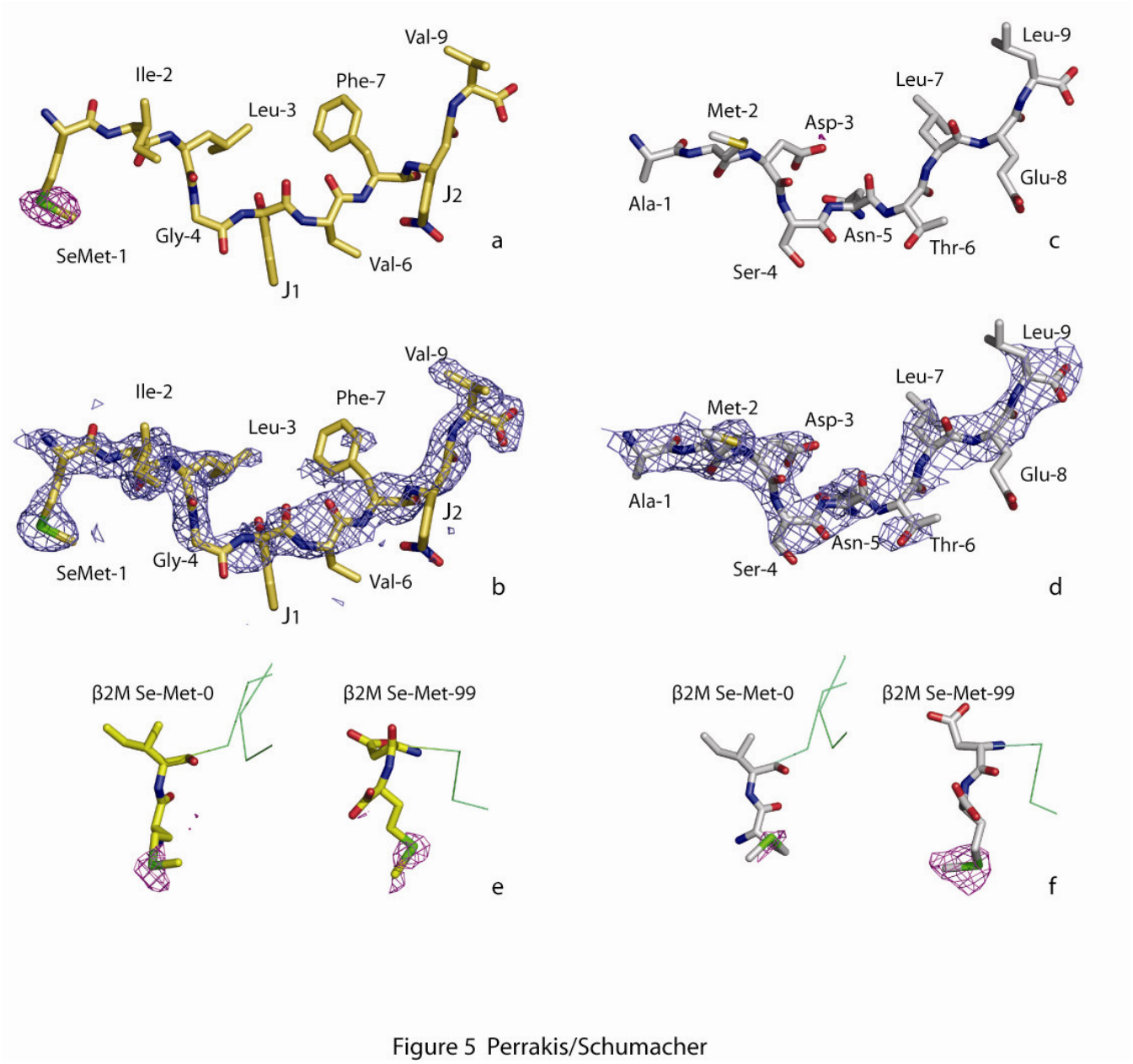

Figure 5 Perrakis/Schumacher

TOC GRAPHICS